行政院國家科學委員會專題研究計畫成果報告

雷射晶體在強居量反轉下的能量轉移機制之研究(2/2)

Study of energy-transfer upconversion in laser crystals at high inversion densities

計畫編號：NSC 90－2112－M－009－034－

執行期限：90 年 8 月 1 日至 91 年 7 月 31 日

主持人：陳永富　交通大學電子物理系

計畫參與人員：黃怡正、李建龍、謝弘道 交通大學電子物理系

一、中文摘要

本計畫利用空間相關速率方程式建立一理論模式來考量能量轉移上轉換對端面激發式Q開關雷射的影響。

關鍵詞：Q開關雷射、熱負載、能量轉移上轉換

Abstract

The influence of energy transfer upconversion (ETU) on diode-end-pumped actively Q-switched lasers is investigated by the space-dependent rate equation analysis. The numerical analysis reveals that as a consequence of the ETU effect there is an optimum pump size for producing the largest pulse energy and a different optimum pump for yield the highest peak power at a given pump power. The practical example of the diode-pumped actively Q-switched Nd:YAG laser has been performed to verify the present model.

Keywords: fractional thermal loading, energy transfer upconversion, Q-switched, Nd:YAG

二、緣由與目的

Diode-pumped solid-state lasers have been shown to be efficient, compact, and reliable all-solid-state optical source. Neodymium-doped laser crystals are widely used in diode-pumped solid-state lasers. Recently, the space-dependent rate equations were used to analyze the performance of diode-pumped actively Q-switched lasers [1]. The theoretical results showed that the output efficiency increases as the pump spot size decreases. However, this conclusion is contradiction to the experimental result for Nd-doped lasers because the effect of energy-transfer upconversion (ETU) was not included in the analysis. The ETU process has a significant influence on the population mechanisms for the Nd-doped laser crystals with high excitation density [2-10]. Since a smaller pump size leads to a higher excitation density during low-Q segment of the cycle, the influence of ETU should be considered to find the optimum pump size in a diode-pumped actively Q-switched laser.

In scaling end-pumped lasers to higher power, the fiber-coupled laser-diodes with circular beam profiles are often used as pump sources because the high power diode lasers are very asymmetric in their emitting aperture dimensions [11,12]. In this work, we developed a theoretical model to consider the influence of ETU on the performance of fiber-coupled diode-end-pumped actively Q-switched lasers. With the numerical analysis, we investigated the optimum pump sizes for maximizing pulse energy and maximizing peak power, respectively. The practical example of Nd:YAG laser was considered to confirm the analysis of the present model.

三、結果與討論

Although the space–dependent rate equations were used in ref. [1], the dependence on the longitudinal axis z was neglected. For end-pumped lasers, the population inversion density is not only a function of radial coordinate r but also a function of z because the pump light intensity in the gain medium is attenuated along the axis z. To take the z-dependence into account, the rate equations during the high-Q segment of the cycle is modified as [1]

$$\int_{\text{cavity}} \frac{d\phi(r,z,t)}{dt}\,dV = \int_{\text{rod}} c\sigma\, n(r,z,t)\phi(r,z,t)\,dV - \frac{\ln(1/R)+L}{t_r}\int_{\text{cavity}} \phi(r,z,t)\,dV \quad , \quad (1)$$

$$\frac{dn(r,z,t)}{dt} = -\gamma c\sigma\, n(r,z,t)\phi(r,z,t) \quad , \quad (2)$$

where $\phi(r,z,t)$ is the intracavity photon density, $n(r,z,t)$ is the population inversion density, σ is the stimulated emission cross section, c is the speed of light in medium, and t_r is the round trip time, γ is the inversion reduction factor, L is the round-trip loss, and R is the

output reflectivity.

Assuming the intracavity photon density to be a Gaussian distribution during the entire formatting process of the Q-switched pulse, the intracavity photon density $\phi(r,z,t)$ can be given by [1]

$$\phi(r,z,t)=\phi_o(t)\exp\left[-\frac{2r^2}{\mu_l^2(z)}\right], \quad (3)$$

$$\mu_l(z)\approx\mu_L \ . \quad (4)$$

Here z_l is the position of the beam waist and the point $z = 0$ is taken to be the incident surface of the gain medium.

Substituting Eq. (3) into Eq. (2) and integrating Eq. (2) over time, we obtain

$$n(r,z,t)=n(r,z,0)\times \exp\left[-\gamma\sigma\int_0^t\phi_o(t)\,dt\exp\left(-\frac{2r^2}{\mu_L^2}\right)\right], \quad (5)$$

where $t = 0$ in Eq. (5) corresponds to the time just at the beginning of the high-Q segment. In other word, $n(r,z,0)$ corresponds to the population inversion density just at the end of the low-Q segment. Therefore, $n(r,z,0)$ can be derived from the rate equation during the low-Q segment of the cycle.

To take the ETU effect into account, the rate equation for population inversion density during the low Q-segment of the cycle is given by [9,13]

$$\frac{dn(r,z,t)}{dt}=R_p(r,z)-\frac{n(r,z,t)}{\tau_s}-\zeta\,n(r,z,t)^2, \quad (6)$$

where $R_p(r, z)$ is the rate of the pump intensity at any radial location r or axial location z, τ_s is the emission lifetime, and ζ is the upconversion rate.

The main difference between the present and the previous model [14] is that the term $\zeta\,n(r,z,t)^2$ is added in Eq. (6) to take the ETU effect into account. From Eq. (6), the initial population inversion density just at the end of the low-Q segment at the repetition rate f can be derived as

$$n(r,z,0)=\frac{2\tau_s R_p(r,z)}{A(r,z)+1}\times \left\{\frac{1-\left[\frac{A(r,z)+1}{A(r,z)-1}\right]\left[\frac{A(r,z)-B(r,z)-1}{A(r,z)+B(r,z)+1}\right]\exp\left[-\frac{A(r,z)}{\tau_s f}\right]}{1+\left[\frac{A(r,z)-B(r,z)-1}{A(r,z)+B(r,z)+1}\right]\exp\left[-\frac{A(r,z)}{\tau_s f}\right]}\right\} \quad (7)$$

$$A(r,z)=\sqrt{1+4\tau_s^2\,\zeta\,R_p(r,z)}, \quad (8)$$

$$B(r,z)=2\tau_s\,\zeta\,n_f(r,z) \ , \quad (9)$$

where $n_f(r,z)$ is the residual population inversion density from the preceding pulse. Eq. (7) indicates that when the pump power is high enough, i.e., $A(r,z)>>B(r,z)$, the residual population inversion density can be neglected. At high pump power, Eq. (7) then becomes

$$n(r,z,0)=\frac{2\tau_s R_p(r,z)}{A(r,z)+1}\times \left\{\frac{1-\exp\left[-\frac{A(r,z)}{\tau_s f}\right]}{1+\left[\frac{A(r,z)-1}{A(r,z)+1}\right]\exp\left[-\frac{A(r,z)}{\tau_s f}\right]}\right\} . \quad (10)$$

On the other hand, at low repetition rate, i.e., $\tau_s f<<1$, Eq. (7) can be simplified as

$$n(r,z,0)=\frac{2\tau_s R_p(r,z)}{A(r,z)+1} \ . \quad (11)$$

Clearly, $n(r,z,0)$ at low repetition rate is independent of the repetition rate because the spontaneous emission results in the saturation of the inversion density. Since the influence of the ETU effect is greatly crucial at high pump powers and low repetition rates in the Q-switched operation [9], Eq. (11) is employed for the further analysis.

The beam profile of a fiber-coupled laser diode can be approximately described as a top-hat distribution [11,12]:

$$R_p(r,z)=\frac{P_{abs}}{h\nu_p}\frac{1}{\pi\mu_p^2}\frac{\alpha\exp(-\alpha z)}{1-\exp(-\alpha l)}\Theta\left(\mu_p^2-r^2\right), \quad (12)$$

where α is the absorption coefficient at the pump wavelength, l is the length of the crystal, μ_p is the averaged pump size in the active medium, P_{abs} is the absorbed pump power, $h\nu_p$ is the pump photon energy, and $\Theta(\ )$ is the Heaviside step function.

Substituting Eqs. (3) (5), (11) and (12) into Eq. (1), performing the integration over the space and defining the parameters,

$$\tau=\frac{t}{t_r}\left[\ln(1/R)+L\right] \ , \quad (13)$$

$$\Phi(\tau)=\frac{\gamma\sigma\phi_o(t)}{\left[\ln(1/R)+L\right]/t_r} \ , \quad (14)$$

$$=\frac{4\pi\tau_s^2\alpha}{\pi\mu_p^2\left(1-e^{-\alpha l}\right)}\frac{P_{abs}}{h\nu_p} \ , \quad (15)$$

$$G = \frac{2\pm}{\pi\mu_p^2}\frac{P_{abs}\tau_s}{h\nu_p}\frac{1}{\ln(1/R)+L}g(\gamma) \quad , \tag{16}$$

and

$$g(\gamma) = \frac{2}{(1-e^{-\alpha l})}\left\{2\left(\sqrt{1+\gamma}-\sqrt{1+\gamma e^{-\alpha l}}\right) + \ln\left[\frac{e^{-\alpha l}\left(2+\gamma-2\sqrt{1+\gamma}\right)}{2+\gamma e^{-\alpha l}-2\sqrt{1+\gamma e^{-\alpha l}}}\right]-\alpha l\right\} \tag{17}$$

, we obtain

$$\frac{d\Phi(\tau)}{d\tau} = G\frac{\Phi(\tau)}{F(\tau)}\left\{\exp\left[-F(\tau)\exp\left(-\frac{2\mu_p^2}{\mu_L^2}\right)\right]-\exp[-F(\tau)]\right\}-\Phi(\tau) \tag{18}$$

where

$$F(\tau) = \int_0^{\tau}\Phi(\tau')d\tau' \quad . \tag{19}$$

The function $g(\gamma)$ defined in Eq. (17) represents the fraction of excited ions that involve the lasing process. In other words, $1-g(\gamma)$ represents the fractional reduction of the population inversion that is due to the ETU effect. Using the fact that $\alpha l >> 1$ for ensuring sufficient absorption of the pump beam, $g(\gamma)$ can be simplified as

$$g(\gamma) = \frac{2}{\gamma}\left\{2\left(\sqrt{1+\gamma}-1\right)+\ln\left[\frac{4\left(2+\gamma-2\sqrt{1+\gamma}\right)}{\gamma^2}\right]\right\} \tag{20}$$

Note that Eq. (20) is quite similar to the equation derived by Hardman *et al.* who reported that the ETU effect leads to a notable difference in the thermal lens between lasing and nonlasing conditions [7]. The main difference between Eq. (20) and the equation given by Hardman *et al.* is that the top-hat distribution instead of Gaussian distribution was used in the present derivation. If $\beta = 0$, i.e. there are no ETU effects, one can find $\lim_{\gamma\to 0} g(\gamma) = 1$. In fact, the parameter γ defined in Eq. (15) is a measure of the magnitude of the ETU effect. Fig. 1 plots the dependence of $g(\gamma)$ on the parameter γ for the example of $\alpha l = 3$. It can be found that $g(\gamma)$ is a decreasing function of γ. Therefore, decreasing γ is the key to the reduction of ETU effect. From Eq. (15), expanding pump size can lead to a decrease in γ. However, a larger pump size may result in not only a higher threshold but also a worse overlapping efficiency. Therefore, the optimum pump-to-mode size ratio is expected when these two effects are balanced.

In terms of $\Phi(\tau)$, the expressions for the peak output power P_{po} and the output pulse energy E_o are given by [1,15]

$$P_{po} = \frac{\pi\mu_L^2 h\nu}{4\pm\tau_r}\left[\ln\left(\frac{1}{R}\right)+L\right]\ln\left(\frac{1}{R}\right)\Phi_m \quad , \tag{21}$$

$$E_o = \frac{\pi\mu_L^2 h\nu}{4\pm\tau_r}\ln\left(\frac{1}{R}\right)\Phi_{\text{integ}} \quad , \tag{22}$$

where Φ_m is the maximum value of $\Phi(\tau)$ and $\Phi_{\text{integ}} = \int_0^{\infty}\Phi(\tau)d\tau$. Therefore, as long as $\Phi(\tau)$ is solved from Eqs. (18) and (19), the peak output power and the output pulse energy can, respectively, be determined from Eqs. (21) and (22). To illustrate the dependence of the ETU effect on the pump size, we use the parameters: $\pm = 2.8\times10^{-19}\ \text{cm}^2$ [15], $\beta = 2.8\times10^{-16}\ \text{cm}^3/\text{s}$ [2], $\alpha = 7\ \text{cm}^{-1}$, $\mu_o = 0.3\ \text{mm}$, L = 0.005, R = 0.70, and τ=230 μs and employ the Runge-Kutta method to solve Eqs. (18) and (19). The parameters used here corresponds to a typical 1.0 at.% Nd:YAG laser. Fig. 2 shows the calculated results for Φ_{integ} as a function of the pump size for several absorbed pump powers. For comparison, we also plot the results computed without the ETU effect in the same figures. Fig. 2 reveals that the pulse energy without the ETU effect almost unchanged for a given pump power as the pump size is sufficiently small. However, considering the ETU effect there is an optimum pump size for the output pulse energy because smaller pump sizes, leading to higher excitation densities, increase the fractional reduction of the population inversion. Fig. 2 also shows that the optimum pump size increases with increasing the pump power.

Fig. 3 depicts the calculated results for Φ_m as a function of the pump size for several absorbed pump powers. It can be seen that without the ETU effect a smaller pump size can result in a higher output peak power. However, as a result of the ETU effect there is an optimum pump size for the peak power. Fig. 3 reveals that the peak power decreases dramatically as the pump size is smaller than the optimum value. Making a comparison between the results of Figs. 2 and 3, it can be found that at a given pump power the value of the optimum pump size for maximizing pulse energy is clearly smaller than the result for maximizing peak power. The reason is due to the fact that a higher inversion density leads to a larger stimulated emission within the high-Q

segment and then a higher peak power.

四、 結論

We have included the ETU effect into the space-dependent rate-equation analysis to study the optimum pump size in the diode-end-pumped actively Q-switched laser. With the theoretical model, the dependence of the output performance on the pump size was numerically calculated for different pump power. The calculated results reveal that without the ETU effect a smaller pump size basically results in a better output performance. However, as a result of the ETU effect, there is an optimum pump size for producing the largest pulse energy and a different optimum pump for obtaining the highest peak power. In general, the optimum pump size is an increasing function of the pump power. The practical example of the diode-pumped actively Q-switched Nd:YAG laser has been performed to verify the present model. We believe that the present model can be applied to other Nd-doped laser materials and used to optimize the actively Q-switched laser.

五、參考文獻

[1] X. Zhang, S. Zhao, Q. Wang, B. Ozygus, and H. Weber, IEEE J. Quantum Electron. vol. 35, pp.1912-1918, 1999.

[2] Y. Guyot, H. Manan, J. Y. Rivoire, R. Moncorgé, N. Garnier, E. Descroix, M. Bon, and P. Laporte, Phys. Rev. B **51**, pp. 784-799, 1995.

[3] S. A. Payne, G. D. Wilke, L. K. Smith, and W. F. Krupke, Opt. Commun. **111**, pp. 263-268, 1994.

[4] J. L. Doualan, C. Maunier, D. Descamps, J. Landais, and R. Moncorge, Phys. Rev. B 62, pp. 4459-4463, 2000.

[5] D. L. Russell, and K. Holliday, Optics. Commun. **191**, pp. 277-294, 2001.

[6] V. Ostroumov, T. Jensen, J. P. Meyn, G. Huber, and M. A. Noginov, J. Opt. Soc. Amer. B **15**, pp. 1052-1060, 1998.

[7] M. Pollnau, D. R. Gamelin, S. R. Luthi, H. U. Gudel, and M. P. Hehlen, Phys. Rev. B 61, pp. 3337-3346, 2000.

[8] Y. F. Chen, Y. P. Lan, and S. C. Wang, IEEE J. Quantum Electron. vol. 36, 615-619, 2000.

[9] Y. P. Lan, Y. F. Chen, and S. C. Wang, Appl. Phys. B71, pp. 27-31, 2000.

[10] L. C. Courrol, E. P. Maldonado, L. Gomes, N. D. Vieira Jr., I. M. Ranieri, S. P. Morato, Optical Materials 14, pp. 81-90, 2000.

[11] Y. F. Chen, T. M. Huang, C. F. Kao, C. L. Wang, and S. C. Wang, IEEE J. Quantum Electron. vol. **33**, pp. 1424-1429, 1997.

[12] Y. F. Chen, IEEE J. Quantum Electron. vol. **35**, pp. 234-239, 1999.

[13] Y. F. Chen, J. Opt. Soc. Am. B.17, pp.1835-1840, 2000.

[14] R. B. Chesler, M. A. Karr, and J. E. Geusic, Proceddings of The IEEE, vol. 58, pp. 1899-1914, 1970.

[15] W. Koechner, *Solid-State Laser Engineering*, 4th ed. (Springer-Verlag, New York, 1996), p.51

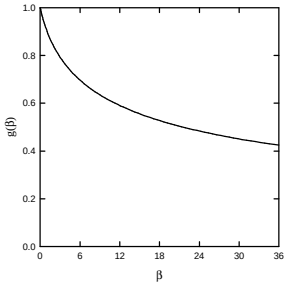

Fig. 1

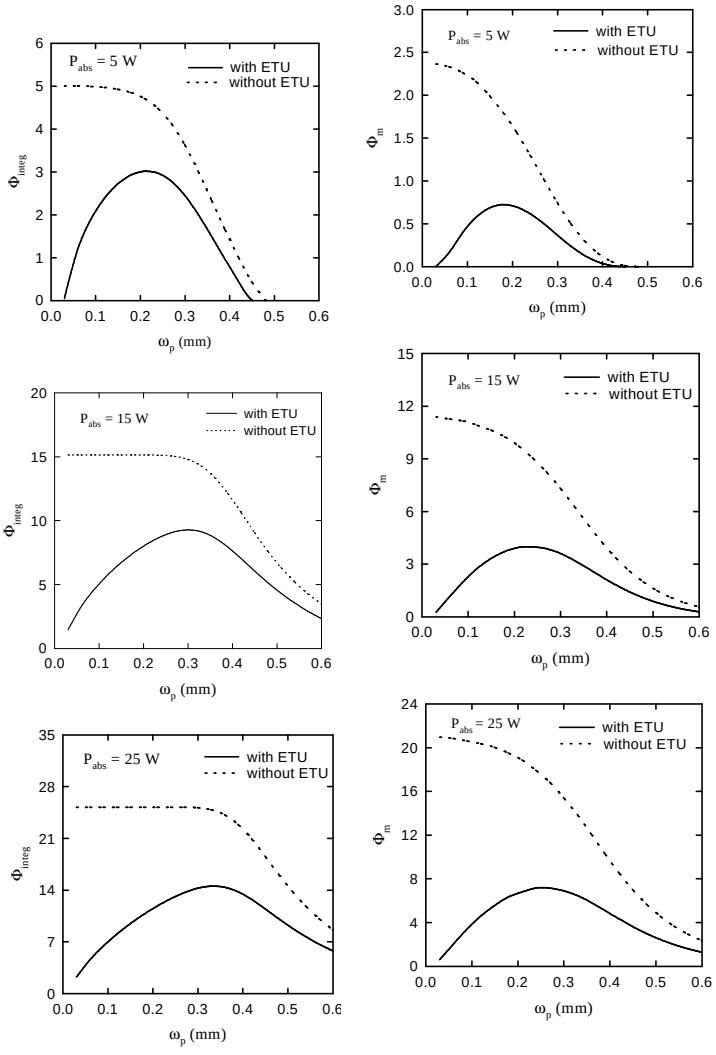

Fig. 2

Fig. 3

行政院國家科學委員會補助專題研究計畫成果報告

※※※※※※※※※※※※※※※※※※※※※※※※※※
※　　　　　　　　　　　　　　　　　　　　　　　　※
※雷射晶體在強居量反轉下的能量轉移機制之研究(2/2)※
※　　　　　　　　　　　　　　　　　　　　　　　　※
※※※※※※※※※※※※※※※※※※※※※※※※※※

計畫類別：■個別型計畫　　□整合型計畫
計畫編號：NSC 90－2112－M－009－034－
執行期間：90 年 8 月 1 日至 91 年 7 月 31 日

計畫主持人：陳 永 富
共同主持人：
計畫參與人員：黃怡正、李建龍、謝弘道

本成果報告包括以下應繳交之附件：
□赴國外出差或研習心得報告一份
□赴大陸地區出差或研習心得報告一份
□出席國際學術會議心得報告及發表之論文各一份
□國際合作研究計畫國外研究報告書一份

執行單位：國立交通大學電子物理系

中　華　民　國　91 年　9　月　26　日